REPORT DOCUMENTATION PAGE

Form Approved
OMB No. 0704-0188

1. REPORT DATE *(DD-MM-YYYY)*	2. REPORT TYPE	3. DATES COVERED *(From - To)*
JUNE 2013	JOURNAL ARTICLE (Post Print)	JUL 2012 – NOV 2012

4. TITLE AND SUBTITLE

GENERATION OF HIGH PURITY ENTANGLED PHOTON-PAIR IN A SHORT HIGHLY NON-LINEAR FIBER

5a. CONTRACT NUMBER

5b. GRANT NUMBER FA8750-12-1-0136

5c. PROGRAM ELEMENT NUMBER N/A

6. AUTHOR(S)

Yong Meng Sua, John. Malowicki, Masaaki Hirano, Kim Fook Lee

5d. PROJECT NUMBER T2HC

5e. TASK NUMBER MT

5f. WORK UNIT NUMBER EC

7. PERFORMING ORGANIZATION NAME(S) AND ADDRESS(ES)

MICHIGAN TECHNOLOGICAL UNIVERSITY
1400 Townsend Dr
Houghton MI 49931-1200

8. PERFORMING ORGANIZATION REPORT NUMBER

N/A

9. SPONSORING/MONITORING AGENCY NAME(S) AND ADDRESS(ES)

Air Force Research Laboratory/Information Directorate
Rome Research Site/RITE
525 Brooks Road
Rome NY 13441-4505

10. SPONSOR/MONITOR'S ACRONYM(S)

AFRL/RI

11. SPONSORING/MONITORING AGENCY REPORT NUMBER

AFRL-RI-RS-TP-2013-026

12. DISTRIBUTION AVAILABILITY STATEMENT

APPROVED FOR PUBLIC RELEASE; DISTRIBUTION UNLIMITED. PA Case Number: 88ABW-2012-0609
DATE CLEARED: 19 NOV 2012

13. SUPPLEMENTARY NOTES

14. ABSTRACT

We generate photon pairs at telecom wavelength through a spontaneous four-wave mixing process in a short 10 m of highly nonlinear fiber. We use a counterpropagating scheme to generate a correlated and entangled photon pair. We observe coincidence to accidental-coincidence ratio of 29±3 at room temperature (300 K) and as high as 130±5 when the fiber is cooled to liquid-nitrogen temperature (77 K). Two-photon interference with visibility >98% (>92%) and the violation of Bell's inequality by >12 (≈5) standard deviation are observed at 77 K (300 K), respectively, without subtracting accidental-coincidence count. We obtain a photon-pair production rate about factor 3(2) higher than a 300 m dispersion-shifted fiber at 300 K (77 K).

15. SUBJECT TERMS

Entangled photon-pair, Highly Nonlinear Fiber, Quantum communication

16. SECURITY CLASSIFICATION OF: a. REPORT	b. ABSTRACT	c. THIS PAGE	17. LIMITATION OF ABSTRACT	18. NUMBER OF PAGES	19a. NAME OF RESPONSIBLE PERSON
					JOHN MALOWICKI
U	U	U	UU	05	19b. TELEPHONE NUMBER (*Include area code*) N/A

Standard Form 298 (Rev. 8-98)
Prescribed by ANSI Std. Z39.18

Optics Letters, Vol 38, Issue 1, pp. 73-75

Generation of high purity photon-pair in a short highly non-linear fiber

Yong Meng Sua,[1] John Malowicki,[2] Masaaki Hirano,[3] and Kim Fook Lee[1,*]

[1] *Department of Physics, Michigan Technological University, Houghton, MI 49931*
[2] *Air Force Research Lab, Rome NY 13441*
[3] *Optical Communications R&D Labs., Sumitomo Electric Industries, ltd., Tsukuba, Japan.*
**Corresponding author: kflee@mtu.edu*

We generate photon pairs at telecom wavelengths through a spontaneous four-wave mixing process in a short 10 meter highly nonlinear fiber (HNLF). We use a counter propagating scheme to generate correlated and entangled photon-pairs. We observe a coincidence count to accidental coincidence count ratio (CAR) of 29±3 at room temperature (300° K) and as high as 130±5 when the fiber is cooled to liquid-nitrogen temperatures (77° K). Two photon interference with visibility >98% (>92%) and Bell's inequality violation by >12 (≈5) standard deviations of measurement uncertainty are observed at 77° K (300° K) without subtracting accidental-coincidence counts.

OCIS Codes: 270.0270, 270.5585, 190.4370

Entangled photon pair sources at telecom wavelengths are essential for the implementation of quantum information processes such as quantum key distribution [1] and quantum metrology [2]. Entangled photon pair generation via spontaneous parametric down conversion (SPDC) was first observed in $\chi^{(2)}$ nonlinear crystal [3]. However, the compatibility of a nonlinear crystal source with fiber and waveguide based telecommunication infrastructure is limited by its dispersive nature and inherently poor spatial mode. Therefore, direct generation of entangled photon pairs in optical fiber attracted enormous interest due to its better spatial mode definition and inherent compatibility with existing fiber optics technologies for long distance transmission, storage and processing. Entangled photon pair generation in optical fiber is realized via spontaneous four-waves mixing (SFWM) and more recently in periodically poled fiber through SPDC [5-8]. While the initial success of entangled photon pair generation through SPDC in periodically poled fiber is exciting, the compatibility of this fiber with standard transmission fiber remains challenging [8]. Entangled photon pair generation via SFWM was successfully demonstrated with dispersion shifted fiber (DSF) [5] and highly nonlinear microstructure fiber (HNMSF) [7]. In contrast, entangled photon pair generation at telecom wavelengths via SFWM using highly nonlinear fiber (HNLF) has yielded relatively little success [9]. In addition, it is claimed that the higher Raman noise photons due to the Germanium oxide doping in HNLF deteriorate its performance compared to DSF and HNMSF [10]. Nonetheless, it is also shown that Raman noise photons can be reduced by appropriate detuning of the photon pair detection band [11] and cooling the fiber [5, 12].

In this paper, we demonstrate the generation of polarization entangled photon pairs at telecom wavelength via SFWM using a dispersion shifted highly nonlinear fiber (HNLF). The polarization entangled photon pairs are created by adopting a compact counter propagating scheme (CPS) as shown in Fig.1.

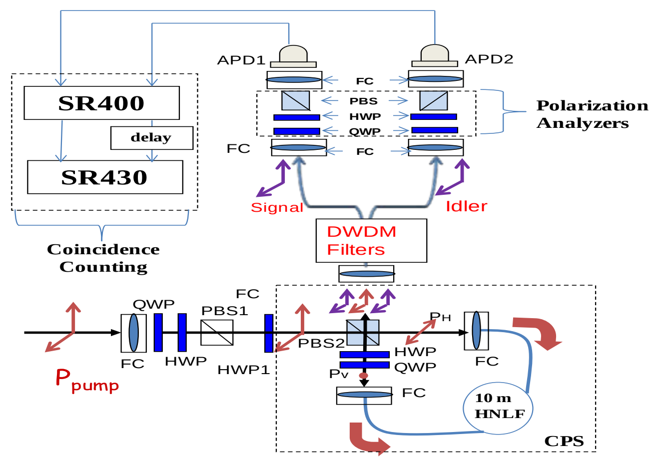

Fig. 1. Layout of the experimental setup. FC, fiber-to-free space collimators; PBS, polarization beam splitter; HWP, QWP, half- and quarter-wave plates; DWDM, dense wavelength division multiplexer; APD, Avalanche photodiode.

A 10 m long HNLF fabricated by Sumitomo with a core diameter of 4 microns is fusion spliced to a single mode fiber for a measured total loss of less than 1 dB, demonstrating excellent compatibility with standard transmission fiber. The HNLF's zero dispersion wavelength is engineered to be at 1555 nm, has a high nonlinear coefficient γ of 30 W/km, attenuation of 0.9 dB/km, and 8.5 microns square effective area. The γ value of this HNLF is significantly higher than that of conventional nonlinear fiber (≈10 W/km) and dispersion shifted fiber (≈2 W/km) [10]. The pump pulse at 1554.1 nm with the pulse duration ≈ 5 ps and repetition rate of 46.5 MHz is spectrally carved out from a mode-locked femtosecond fiber laser using a 1 nm bandwidth Dense Wavelength Division Multiplexer (DWDM) filter. In order to achieve the required power, the pump pulses are further amplified using an Erbium-doped-fiber-amplifier. The amplified spontaneous emission from the Erbium-doped-fiber-amplifier is suppressed by utilizing another two cascaded 1 nm DWDM filters.

The pump pulses are launched via fiber-to-free space collimators and go through a quarter wave plate (QWP) and half wave plate (HWP) to compensate for changes of the polarization states of the pump pulses due to the fiber birefringence. The pump pulses pass through a PBS to ensure the input pump is horizontally polarized. HWP1 at 22.5 degree is inserted in front of the PBS2 to divide the pump pulses equally into horizontally and vertically polarized components for creating polarization entanglement. Horizontally and vertically polarized pump pulses propagate through the HNLF in clockwise and counterclockwise directions and emerge from the same output port of the PBS2 along with the scattered signal and idler photon pairs. QWP and HWP in the CPS are utilized to compensate the birefringence induced polarization changes of the signal and idler photons. Bandwidth DWDM filters of 1 nm at 1560.6 nm and 1447.7 nm are used to separate the signal and idler photons with 6.5 nm detuning from the pump wavelength, as well as suppress the pump pulses with isolation of more than 110 dB. Proper detuning of the signal and idler photon detection band helps to reduce leakage of pump photons and scattered Raman photons [11]. The outputs photons from the signal and idler channels are guided through the polarization analyzers consisting of a quarter-wave plate, a half-wave plate and a polarizing beam splitter. Note that the polarizing beam splitter in the polarization analyzers will filter out the cross-polarized scattered Raman photons. On the other hand, the co-polarized scattered Raman photons can be reduced by cooling the HNLF [5, 11]. Stoke and anti-Stokes Raman scattering photons are proportional to the Bose population factors $n_{th} + 1$ and n_{th} [13]. The Bose population factor is given as $n_{th} = 1/\left[exp\left(\frac{h}{kT}\frac{c\Delta\lambda}{\lambda^2}\right) - 1\right]$, where $\Delta\lambda$ is the detuning from the pump wavelength, λ is the pump wavelength, T is the HNLF temperature, c is the light velocity in fiber, h is Planck's constant and k is Boltzmann's constant. Theoretical calculation shows that when the HNLF is cooled to 77° K the Bose population factor of Raman photons is reduced by a factor of 4 compared to 300° K.

With the appropriate combination of the quarter-wave plate and half-wave plate orientations, the signal and idler photons of the desired polarization state will arrive to the avalanche photodiodes (APD) with negligible loss. Signal and idler photons are detected by fiber coupled InGaAs/InP avalanche photodiodes (Princeton Lightwave, PGA-300) operated in gated Geiger mode at room temperature. The APDs are gated by 1 ns FWHM gate pulses at the rate of 728 kHz, which are triggered from the pump laser pulses at 1/64 frequency-division. The timing of gate pulses for each APD can be independently adjusted by digital delay generators to coincide with the arrival of the signal and idler photons at the APDs. In gated Geiger mode, quantum efficiency, dark counts probability and FWHM detection window of APD1 (APD2) are about 10.3% (9.8%), 2.5×10^{-3} (2.2×10^{-3}) and 280 ps (250 ps). Total detection efficiencies of signal and idler photon are about 4.99% and 4.87% respectively, including propagation losses of optical components, splicing losses of the HNLF and the APDs quantum efficiencies. The coincidence counting system consisting of the Dual Channel Gated Photon Counter (SR400), delay pulse generator (HP811A) and Multi Channel Scaler (SR430) are used for the coincidence detection. A coincidence count will be recorded when both APDs detected a photon at the same gated time interval while an accidental coincidence count is recorded when the APDs detected a photon at the adjacent gated time interval.

Coincidence counts to accidental coincidence counts ratio (CAR) is used to determine the quality of a correlated photon source, with a high CAR value indicating a high purity correlated photon source. For the CAR measurement, HWP 1 is oriented with only horizontally polarized pump pulses entering the CPS and propagates through the HNLF. Proper orientation of the QWP and HWP in the CPS will warrant that scattered signal and idler photons remain in the horizontal polarized state and emerge through the output port of PBS2. The polarization analyzers are adjusted in such a way that horizontally polarized signal and idler photons will pass through to APD1 and APD2.

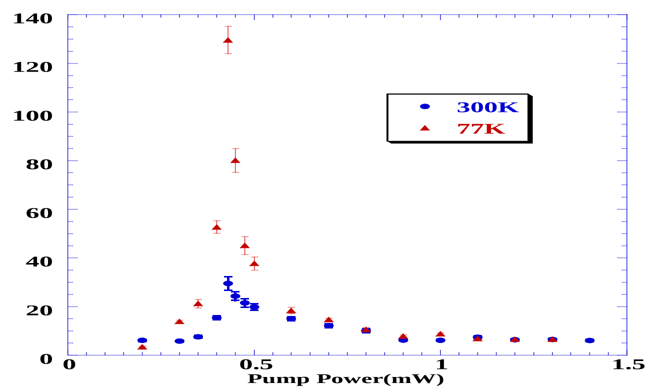

Fig. 2. Coincidence count to accidental coincidence count ratio (CAR) versus pump power with HNLF at 300° K (Blue dot) and 77° K (Red triangle).

CAR measurements are performed at both 300° K and 77° K. The dispersion shifted HNLF in a plastic buffer coating is cooled to 77° K by immersing it into liquid nitrogen filled Dewar. Advancement of photon arrival times by about 130 ps indicates contraction in fiber length when the HNLF is cooled to 77° K. It is also noted that the zero dispersion wavelength of the HNLF is shifted toward the shorter wavelengths at 77° K. Figure 2 shows the measurement of CAR for different pump powers at 300° K and 77° K. CAR values of about 29 and 130 are obtained at 300° K and 77° K respectively, both with pump power of 430 μW. The trend observed for CAR measurements at both temperatures are similar to those obtained by other entangled photons sources [5, 8, and 14]. We believe that low CAR values at low pump powers are due to the limitation of the detection efficiencies of the APDs. While low CAR values at high pump powers could be attributed to the noise photons from the leakage of pump photons through the cascaded DWDM filters. On top of that, multi-photons effect that arises from generation of more than a pair of the correlated photons at high pump power could lead to low a CAR values. It is noticed that CAR values at 77° K are significantly higher than at 300° K. We believe that a reduced Raman scattering process at 77° K is the main factor that contributed to the much improved CAR values. As the fiber is cooled to 77° k the Bose population factor is expected to be reduced by a factor of 4 compared to 300° K, which is approximately the 4.5 times higher CAR value at 77° K that is observed in our experiment.

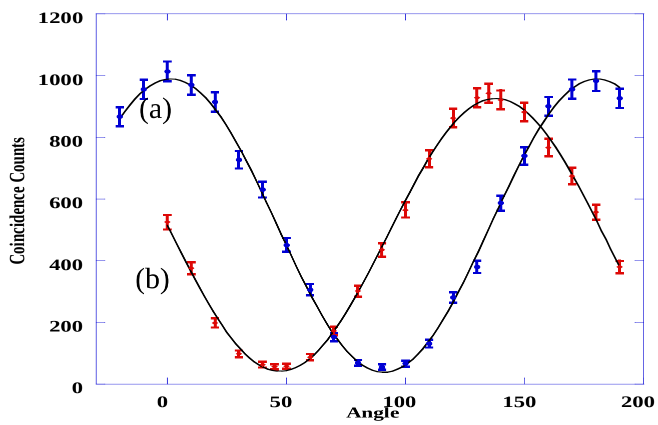

Fig. 3. Two-photon interference fringes with HNLF at 300° K (a) θ_1= 0° and (b) θ_1= 135°.

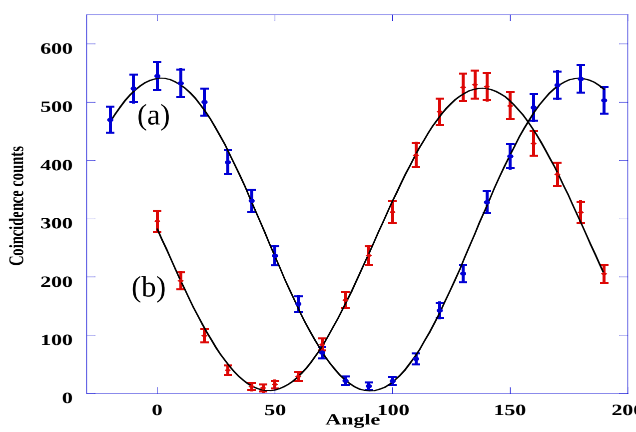

Fig. 3. Two-photon interference fringes with HNLF at 77K (a) θ_1= 0° and (b) θ_1= 135°.

We then created the polarization entangled state $|\Psi_i\rangle = |H_i\rangle|H_s\rangle + e^{2i\phi_p}|V_i\rangle|V_s\rangle$ with HNLF using the counter propagating scheme, where ϕ_p is the relative phase between the horizontally and vertically polarized pump pulses. HWP 1 at 22.5 degree is inserted in front of PBS2 to equally divide the pump pulses into horizontal and vertical polarized components at 430 μW, which is the optimal power determined from the CAR measurement. With the low probability of the spontaneous four-wave mixing process, it is unlikely that each pump pulse will scatter more than a pair of signal and idler photons. Horizontally and vertically polarized signal idler photon pairs propagate through the same optical path in clockwise and counterclockwise directions and emerge from the same output port of the PBS2 with the probability amplitude of $|H_i\rangle|H_s\rangle$ and $|V_i\rangle|V_s\rangle$ each. The fidelity of the entangled two-photon state is examined by measuring the two photon interference fringe of the signal and idler photons. For this experiment, the polarization analyzers at the signal and idler channel are set to θ_1 and θ_2 for the detection of the entangled two-photon state. We set θ_1= 0° and θ_1=135° at the signal channel and vary θ_2 at the idler channel, then record the coincidence counts between the two channels as well as single counts of both channels for about 68 s. Two-photon interference measurements with HNLF at 300° K and cooled to 77° K are shown in Fig 3 and Fig 4 respectively. At 300° K, two-photon interference fringe with a visibility of more than 92% is observed, while visibility of more than 98% is obtained when HNLF is cooled to 77° K. The lower visibility at 300° K is likely due to the contamination of Raman photons that give rise to accidental coincidence counts. On the other hand, higher visibility at 77° K is primarily prohibited by the imperfection in optical components, poor detection efficiencies of the detectors and the remaining background noise photons. All these measurements are obtained without subtracting the accidental coincidence counts that are due to Raman or any background noise photons, and only detector dark counts are subtracted. The coincidence counts detection rate is mainly limited to the slow detection rate of the single photon detectors and coincidence detection system used in our experiment.

Table 1. Violation of Bell's inequality for state $|H_i\rangle|V_s\rangle - |V_i\rangle|H_s\rangle$

Temperature (K)	$\|S\|$	Violation
300	2.27 ± 0	4.95σ
77	2.79 ± 0.06	12.31σ

Finally, Bell's inequality violation test is performed to verify the non-locality of the polarization entanglement produced with the HNLF. Coincidence counts of 16 different combination analyzer settings with θ_1 = 0°, 90°, -45°, 45°, and θ_2 = -22.5°, 67.5°, 22.5°, 112.5° are recorded for Bell state $|H_i\rangle|V_s\rangle - |V_i\rangle|H_s\rangle$. Next we calculate the Clauser, Horne, Shimony, and Holt form of Bell's inequality, the $|S|$ parameters [15], which comply, $|S| \le 2$ with any local realistic system. The measurement of Bell's inequality violation for HNLF at 300° K and 77° K are shown in Table 1. At 300° K we obtained $|S| = 2.27 \pm 0.054$, which violates Bell's inequality by close to 5 standard deviations. When the HNLF is cooled to 77° K, $|S| = 2.79 \pm 0.064$ which violates Bell's inequality by more than 12 standard deviations is observed.

In conclusion, we demonstrated the generation of telecom wavelength polarization entangled photon pairs in a 10 m dispersion shifted HNLF (γ = 30 W/km) via spontaneous SFWM using compact a CPS. The HNLF polarization entangled photon source exhibits high TPI visibility (>98%) and Bell's inequality violation by more than 12 standard deviations by cooling the fiber to 77° K. Along with the advances in laser source and detection system, we believe the HNLF based polarization entangled source could realize the implementation of efficient quantum system such as quantum key distribution and quantum information processing.

ACKNOWLEDGMENT OF SUPPORT AND DISCLAIMER

(a) The Contractor acknowledges the Government's support in the publication of this paper. This material is based upon

research sponsored by AFRL under agreement number FA8750-12-1-0136.
(b) The views and conclusions contained herein are those of the authors and should not be interpreted as necessarily representing the official policies or endorsements, either expressed or implied, of Air Force Research Laboratory or the U.S. Government.

References

[1] A. K. Ekert, J. G. Rarity, P. R. Tapster, and G. Massimo Palma, Phys. Rev. Lett. 69, 1293 (1992)
[2] V. Giovannetti, S. Lloyd, and L. Maccone, Phys. Rev. Lett. 96, 010401 (2006).
[3] P. G. Kwiat, K. Mattle, H. Weinfurter, A. Zeilinger, A. V. Sergienko, and Y. Shih, Phys. Rev. Lett. 75, 4337 (1995)
[4] X. Li, P. L. Voss, J. E. Sharping, and P. Kumar, Phys. Rev. Lett.94, 053601 (2005)
[5] K. F. Lee, J. Chen, C. Liang, X. Li, P. L. Voss, and P. Kumar, Opt. Lett. 31, 1905 (2006).
[6] M. Medic, J. B. Altepeter, M. A. Hall, M. Patel, and P. Kumar, Opt. Lett. 35, 802 (2010).
[7 J. Fan, A. Migdall, and L. J. Wang, Opt. Lett., 30, Issue 24, pp. 3368-3370 (2005)
[8] E. Y. Zhu, Z. Tang, L. Qian, L. G. Helt, M. Liscidini, J. E. Sipe, C. Corbari, A. Canagasabey, M. Ibsen, and P. G. Kazansky, Phys. Rev. Lett. 108, 213902 (2012).
[9] A. Almeida, S. Carneiro, N. Silva, N. Muga, and A. Pinto, Proc. IEEE EUROCON Int. Conf. Comput. Tool, Apr. 2011, pp. 1–4.
[10] Qiang Zhou, Wei Zhang, Jie-rong Cheng, Yi-dong Huang, and Jiang-de Peng, Opt. Express 18, 17114-17123 (2010)
[11] Xiaoying Li, Paul Voss, Jun Chen, Kim Lee, and Prem Kumar, Opt. Express 13, 2236-2244 (2005)
[12] Hiroki Takesue and Kyo Inoue, " Opt. Express 13, 7832-7839 (2005)
[13] S. A. E. Lewis, S. V. Chernikov, and J. R. Taylor, Opt. Lett. 24, 1823-1825 (1999)
[14] Takesue H, Tokura Y, Fukuda H, Tsuchizawa T, Watanabe T, Yamada K and Itabashi, Appl. Phys. Lett. 91, 201108 (2007)
[15] J. F. Clauser, M. A. Horne, A. Shimony, and R. A. Holt, Phys. Rev. Lett. 23, 880 (1969).